This is an open access article published under an ACS AuthorChoice License, which permits copying and redistribution of the article or any adaptations for non-commercial purposes.

Environmental Science & Technology

Article

pubs.acs.org/est

Mackinawite (FeS) Reduces Mercury(II) under Sulfidic Conditions

Sharon E. Bone,*[,†,‡] John R. Bargar,[§] and Garrison Sposito[†,‡]

[†]Environmental Science, Policy, and Management, University of California, Berkeley, California 94720, United States

[‡]Geochemistry, Earth Sciences Division, Lawrence Berkeley National Laboratory, Berkeley, California 94720, United States

[§]Stanford Synchrotron Radiation Lightsource, SLAC, 2575 Sand Hill Road, Menlo Park, California 94025, United States

Supporting Information

ABSTRACT: Mercury (Hg) is a toxicant of global concern that accumulates in organisms as methyl Hg. The production of methyl Hg by anaerobic bacteria may be limited in anoxic sediments by the sequestration of divalent Hg [Hg(II)] into a solid phase or by the formation of elemental Hg [Hg(0)]. We tested the hypothesis that nanocrystalline mackinawite (tetragonal FeS), which is abundant in sediments where Hg is methylated, both sorbs and reduces Hg(II). Mackinawite suspensions were equilibrated with dissolved Hg(II) in batch reactors. Examination of the solid phase using Hg L_{III}-edge extended X-ray absorption fine structure (EXAFS) spectroscopy showed that Hg(II) was indeed reduced in FeS suspensions. Measurement of purgeable Hg using cold vapor atomic fluorescence spectrometry (CVAFS) from FeS suspensions and control solutions corroborated the production of Hg(0) that was observed spectroscopically. However, a fraction of the Hg(II) initially added to the suspensions remained in the divalent state, likely in the form of β-HgS-like clusters associated with the FeS surface or as a mixture of β-HgS and surface-associated species. Complexation by dissolved S(-II) in anoxic sediments hinders Hg(0) formation, but, by contrast, Hg(II)−S(-II) species are reduced in the presence of mackinawite, producing Hg(0) after only 1 h of reaction time. The results of our work support the idea that Hg(0) accounts for a significant fraction of the total Hg in wetland and estuarine sediments.

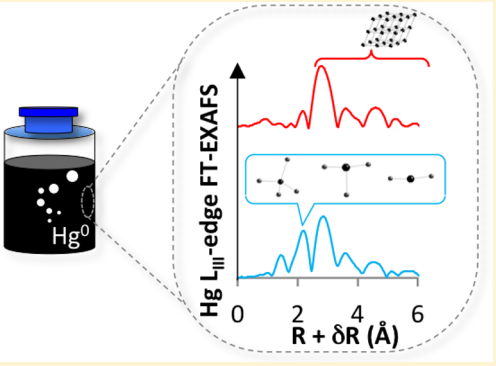

INTRODUCTION

Mercury (Hg) is a contaminant widely distributed in the global environment.[1] Methylation, catalyzed by sulfate-reducing bacteria, Fe(III)-reducing bacteria, or methanogens,[2] is a key chemical transformation of Hg because the metal then can enter food webs as the toxic methyl Hg. The biogeochemical controls on Hg methylation are complex and much of the research has focused on identifying which soluble Hg(II) complexes are bioavailable to methylating bacteria, mainly in sulfidic sediments.[3,4] Neutral Hg(II) complexes are thought to be preferentially methylated because they can passively diffuse into cells where this process occurs.[2,4−7] It has also been shown that Hg-thiol complexes may be actively taken up by cells and subsequently methylated.[8,9]

Conversely, species that pass through the cell membrane less easily are expected to limit Hg methylation. Mercury(II) in either nanocrystalline metacinnabar (β-HgS) or microcrystalline β-HgS is not as available to bacteria as Hg(II) that is nominally dissolved.[10] Reduction of Hg(II) to Hg(0) also may limit Hg methylation in sulfidic sediments. *Dusulfovibrio desulfuricans*, for example, can methylate Hg(0) only after oxidation to Hg(II)-cysteine complexes.[11] Partitioning of Hg(0) within sediments could limit Hg bioavailability: the high vapor pressure and low solubility[12] of Hg(0) suggest that it will either evaporate from sediments or sorb strongly to the sediment matrix.[13]

Dissolved Hg(II)-sulfide [S(-II)] species, which dominate Hg(II) speciation,[3,14] stabilize soluble Hg in the divalent state under anoxic conditions, such that reduction of Hg(II) can occur only in the presence of a powerful reductant. Mackinawite (tetragonal FeS) has been shown to reduce metals under conditions in which the electron activity is high.[15,16] Thus, it is possible that this mineral, which is abundant under the sulfidic conditions where methyl Hg is produced,[17,18] can reduce Hg(II) to Hg(0) or sorb Hg(II), thereby limiting Hg(II) availability to methylating bacteria and consequent toxicity.[10,19] Laboratory incubations of Hg(II) with sediments in batch reactors have demonstrated that the formation of FeS is concurrent with a decrease in the production of methyl Hg.[20−22] The interaction between dissolved Hg(II) and FeS has been investigated previously using molecular methods.[23−25] Although researchers have not reached consensus on the mechanisms of interaction,[24] β-HgS appears to form at high Hg(II):FeS molar ratios, whereas surface complexes of Hg and FeS have been suggested at lower Hg:FeS ratios.[26] Jeong et al.[26] observed that calomel (Hg_2Cl_2) formed from the reaction of Hg(II) with FeS when the Hg:FeS

Received: March 27, 2014
Revised: August 12, 2014
Accepted: August 16, 2014
Published: August 16, 2014

 © 2014 American Chemical Society

ratio was high (>1); however, Hg(II) reduction by FeS has not been observed otherwise.[23,24,26]

We hypothesized that FeS in aqueous suspension can reduce Hg(II) in Hg(II)−S(-II) species to Hg(0) at circumneutral pH and at the Hg:FeS ratios within the range of those observed in anoxic sediments. At the relatively low Hg:FeS ratios employed, we further hypothesized that Hg(II) remaining in our FeS suspensions would be complexed by FeS surfaces. To identify the Hg species produced as a result of the reaction between Hg(II) and FeS, the solid-phase products were characterized using Hg L_{III}-edge extended X-ray absorption fine structure (EXAFS) spectroscopy, while the evolution of purgeable Hg was measured using cold vapor atomic fluorescence spectrometry (CVAFS).

EXPERIMENTAL SECTION

Hg(II) Reaction with FeS. All solutions were prepared inside a Coy vinyl anaerobic chamber under anoxic conditions (0 ppm of O_2, 97% N_2, 3% H_2) using 18.2 MΩ-cm Milli-Q H_2O, degassed by boiling 1 L and then sparging with 95%/5% N_2/H_2 gas (passed through an inline catalyst to remove trace O_2) for 2−3 h.

Solutions were made using ACS reagent-grade chemicals, unless otherwise noted. The S(-II) stock solutions used $Na_2S·9H_2O$ crystals rinsed beforehand to remove any surface contamination present on the crystals. The concentration of S(-II) in the stock solution (ca. 0.5 M) was determined by titration with I_2 according to EPA Method 376.1.[27] The ca. 0.5 M divalent iron [Fe(II)] stock solution comprised Mohr's salt [$(NH_4)_2Fe(SO_4)_2$], with the concentration measured accurately using inductively coupled plasma-optical emission spectrometry (ICP-OES; PerkinElmer Optima 5300 DV). Buffer solutions (10 mM) were prepared using the Good's buffers, MES [2-(*N*-morpholino)ethanesulfonic acid at pH 5.8; MP Biomedicals MES] and HEPES [4-(2-hydroxyethyl)-1-piperazineethanesulfonic acid at pH 6.8], along with Tris [tris(hydroxymethyl)aminomethane at pH 7.8]. The ionic strength of the buffer solutions was increased by adding 0.3 M NaCl. Stock solutions of 0.1 M $Hg(NO_3)_2$ were prepared with degassed 2 M HCl and then diluted in 0.3 M NaCl, 10 mM buffer solution (pH 5.8, 6.8 or 7.8) to achieve a concentration of 0.1 mM Hg. Mercury stock solutions were used in experiments only on the day they were prepared.

Synthesis and processing of Hg-reacted FeS occurred in the anaerobic chamber. An aliquot of the Fe(II) stock solution was added to 0.3 M NaCl, 10 mM buffer solution in anoxic crimp-top glass vials, followed by an aliquot of S(-II) stock solution. Solid-phase FeS was observed to precipitate instantaneously. The FeS suspension was allowed to equilibrate for 5 min before the addition of 0.1 mM Hg(II) stock solution to achieve a final FeS concentration of ca. 1 g/L [ca. 10.5 mM Fe(II) and S(-II)], a final Hg concentration of 4 or 20 μM, and a final suspension volume of 20 mL. The vials were capped using ca. 1 cm thick butyl rubber stoppers and crimped aluminum caps during sample equilibration. Aqueous Fe(II) and S(-II) concentrations were measured for some replicate samples using ferrozine[28] and methylene blue colorimetric methods, respectively, on a PharmaSpec UV-1700 UV−vis spectrometer (Shimadzu). Mackinawite is relatively soluble, so small changes in the initial ratio Fe:S used in its synthesis can lead to relatively large changes in the aqueous Fe and S concentrations. The aqueous Fe(II) concentration (ca. 400−1000 μM) was always in excess of the aqueous S(-II) concentration (from below detection to 15 μM; detection limit, 1.2 μM; Table S4, Supporting Information [SI]). The concentrations of aqueous Fe(II) were somewhat higher, and the concentrations of aqueous S(-II) somewhat lower, than those predicted by FeS solubility.[29,30] X-ray diffraction (Figure S2) and Fe and S K-edge X-ray absorption spectroscopy (Figures S3 and S4) revealed that mackinawite was the only crystalline solid phase present, although some oxidation of the mineral had occurred.[30]

The concentration of Hg(II) used in our study was far greater than typical concentrations found in anoxic sediments, but the ratio of Hg:FeS in the sample suspensions was similar to ratios of Hg:AVS (acid volatile sulfide) observed in the field, assuming that FeS can be equated to AVS and using a range of AVS concentrations in sediments of 2−400 μmol S/g (dry weight)[20] and a range of Hg concentrations in sediments of 0.1−6.5 nmol/g (dry weight),[31] excluding Hg concentrations present in highly contaminated sediments, to obtain a conservative estimate. We calculate the molar ratio of Hg:FeS in sediments to range between 3×10^{-3} and 3×10^{-7}. The molar ratio of Hg:FeS employed in our research ranged between 4×10^{-4} and 2×10^{-3}, which overlaps the high end of the environmentally relevant range.

Thermodynamic calculations (Tables S1 and S2 and Figure S1) were performed using MINEQL+,[32] with component concentrations set equal to those used experimentally. Calculations of the aqueous Hg(II) concentrations were performed for FeS suspensions in both the presence and absence of β-HgS. In both cases it was assumed that FeS dissolution is kinetically facile [which is supported by measurements of FeS dissolution in the presence of Hg(II) at elevated Hg concentrations (5−20 mM)[26]], such that soluble S(-II) is always available to complex Hg(II). Thus, formation of Hg(II)−S(-II) complexes occurs and the intermediate species $S(-II)_{(aq)}$ is immediately replaced through dissolution, even if its nominal concentration in equilibrium with FeS is always low. The Hg(II)−S(-II) species concentrations were always at least 10 orders of magnitude greater than those of Hg(II)−OH or Hg(II)-Cl species. Indeed, the *maximum* concentration of any of the Hg(II)-Cl or Hg(II)−OH complexes was between ca. 10^{-17} and 10^{-23} M (in the absence and presence of β-HgS, respectively), suggesting that reactions between Hg(II)-Cl or Hg(II)-OH complexes and FeS are negligible relative to those between Hg(II)−S(-II) species and FeS.

Hg L_{III}-edge EXAFS Spectroscopy. The samples analyzed using EXAFS spectroscopy were designed to study the impact of three experimental variables on solid-phase Hg speciation: pH, time, and Hg:FeS ratio. Mercury(II)-reacted FeS suspensions were synthesized in buffered solutions at pH 6, 7, or 8 with an initial Hg(II) concentration of 4 or 20 μM and were allowed to equilibrate for 1 or 24 h. X-ray absorption spectra of the solid phases were collected on wet pastes obtained by passing the FeS suspensions through a 0.45 μm filter membrane (inside the anaerobic chamber) the day before analysis and storing them in sealed crimp-top glass vials at −15 °C overnight in a freezer located outside of the anaerobic chamber. The sealed samples were placed on dry ice for transport to the Stanford Synchrotron Radiation Lightsource (SSRL), where they were stored in a freezer until use. Each sample was loaded into a one-slot aluminum sample holder inside an anaerobic chamber before being removed from the anaerobic chamber and plunged directly into liquid N_2, after which they were placed in a liquid He cryostat chamber for measurement at 10 K.

Mercury L_{III}-edge EXAFS spectra were collected at beamline 11-2 at SSRL. The energy of the X-ray beam (uncollimated) was selected using a Si(220) φ = 90 double crystal monochromator detuned by 30% at 12600 eV to minimize harmonics. The fluorescence signal was monitored using a 30-element Ge detector. Between three and eight aluminum foils were placed between the sample and the detector to attenuate Fe Kα fluorescence preferentially. The calibration of the monochromator was monitored throughout collection of the sample spectra using a $HgCl_2$ sample (with the energy of the edge set to 12 284.00 eV).

Between 14 and 20 individual scans individual scans were averaged using the SamView module in SIXPack[33] for each sample and then normalized using the Background Removal module in SIXPack[33] by fitting a linear function to the region between −200 and −50 eV below the edge and a quadratic function to the region between 150 and 900 eV above the edge. The EXAFS spectra [$\chi(k)$] were extracted from the normalized absorption spectra by fitting the region between k = 1 and ca. 10 or 12 Å^{-1} with a spline function. The R_{bkg} value, which determines the upper limit in R-space to which the background function is fit,[34] was >1.0, the default value used by the fitting program,[33] for two samples: pH6_20μMHg_24h and pH8_4μMHg_1h. For these samples, R_{bkg} was increased incrementally until the signal at low R in the Fourier transform of the EXAFS spectrum (FT-EXAFS) was minimized; for both samples the final R_{bkg} value was 1.10 Å.

All fitting was performed using the FEFF EXAFS Fitting module in SIXPack.[33] The theoretical scattering paths that were used to produce the models of the FT-EXAFS spectra were calculated in FEFF 8.2[35] using atomic coordinates derived from Crystal Maker for 7 Å-diameter β-HgS, α-HgS, and α-Hg(0) using the crystallographic structures determined by Wyckoff,[36] Auvrey and Genet,[37] and Barrett et al.,[38] respectively.

Measurement of Purgeable Hg. The concentration of Hg(0) in the absence of FeS was measured using CVAFS to confirm that spurious reduction of Hg(II) does not occur. To this end, controls were synthesized and analyzed which contained only 10 mM HEPES buffer (in 0.3 M NaCl) or H_2O (degassed 18.2 MΩ Milli-Q water) and 20 μM Hg(II), parallel with the samples containing 1 g/L FeS and 20 μM Hg(II). A subset of samples and controls was equilibrated under dark conditions to assess the impact of light on the reduction reaction, since the photoreactivity of soluble Hg(II) is well-known[39] and the samples examined using EXAFS spectroscopy had been equilibrated under illuminated conditions (ambient light). All samples and controls were equilibrated for 24 h. Since Good's buffers may modify the extent of reduction reactions,[40] to test whether the buffers enhanced reduction significantly, experiments were also performed at pH 6 without the addition of buffer (i.e., FeS alone buffered the pH value of the suspension).

The production of purgeable Hg was measured after 24 h in FeS suspensions and control solutions. At the end of a 24-h equilibration period, the samples were purged for 3 h using ultrahigh purity N_2 that was then bubbled through a solution of 600 μM $KMnO_4$ and 8 mM nitric acid to oxidize Hg(0) gas, thus preserving it as Hg(II) for measurement.[41] Before analysis using CVAFS, 300 μL of 4.3 M NH_2OH were added to the preserved samples, which were then diluted in 10 mL of deionized H_2O. An aliquot of the diluted sample was deposited into the bubbler of the CVAFS instrument along with 1 mL of 0.9 M $SnCl_2$ in 1.2 M HCl. Using ultrahigh purity N_2, the $Hg(0)_{(g)}$ generated in the bubbler was deposited onto a gold trap attached to the bubbler with Teflon tubing. Bubbling occurred for 20 min, after which time the gold trap was placed into the heating coil of the dual-gold trap CVAFS instrument, as per EPA method 1631.[42]

The overall detection limit of our procedure to measure purgeable Hg was 0.6 μM, equal to three times the standard deviation of a blank sample containing only degassed 18.2 MΩ Milli-Q water which had been subjected to the same experimental procedure as the samples and which was synthesized and analyzed on five different occasions. This overall detection limit incorporates the error in measurement that arises from purging the initial solution into the $KMnO_4$ solution, reducing the $KMnO_4$ solution, diluting this reduced solution, and measuring the Hg concentration via CVAFS. The concentration of Hg evolved from the control containing H_2O and Hg(II) under illuminated conditions (n = 8; n designates the number of replicate samples) was below the detection limit. The amount of purgeable Hg generated in the controls containing 10 mM HEPES buffer (and 0.3 M NaCl) and Hg(II) under both illuminated ([Hg] = 1.0 ± 0.9 μM, n = 4) and dark conditions ([Hg] = 0.7 ± 0.1 μM, n = 2) was negligible (i.e., approximately equal to the detection limit), with the exception of one of the replicates exposed to light, which contained 2.3 μM purgeable Hg. Although the technique used to measure Hg(0) via CVAFS cannot distinguish between Hg(0) and uncharged aqueous Hg(II) complexes that may be volatilized, we note that although $HgCl_{2(aq)}$ exists in the control containing 10 mM HEPES buffer and 0.3 M NaCl, the concentration of purged Hg measured was close to the detection limit of our technique.

RESULTS

Hg Speciation in the Solid Phase. The X-ray absorption near-edge structure (XANES) spectra of the samples matched that of a published XANES spectrum of Hg(0) measured at 80 K.[43] Furthermore, the positions of the peaks in the first derivatives of the XANES spectra at 12 283, 12 292, and 12 298 eV match those reported previously for Hg(0)[43] (Figure S7). Additionally, the FT-EXAFS spectra exhibited a large peak centered at ca. $R + \delta R$ = 2.7 Å (Figure 1) consistent with that published for α-Hg(0) by Jew et al.[44] In the EXAFS spectrum of sample pH8_20μMHg_24h, α-Hg(0) was the only phase that could be discerned (Figure 1; plots of $\chi(k)k^3$ are provided in Figure S9 of the SI), as indicated by the absence of peaks in the FT-EXAFS spectrum at or below ca. $R + \delta R$ = 2 Å, which would indicate bonding between Hg and an anion. This latter spectrum was then fit assuming that the sample contained solely Hg(0) in order to determine the amplitude reduction factor (S_0^2) and Debye−Waller factors (σ^2, Å^2) for Hg(0)-Hg(0) scattering paths. The amplitude reduction factor is correlated with the Debye−Waller factor; however, S_0^2 is independent of k, whereas σ^2 is dependent upon k.[45] Thus, the EXAFS spectrum was fit using differing k-weights to increase the precision of the fitted S_0^2 and σ^2 parameters[45] (Figure S8 of the SI). The fitted parameters (Table S5, of the SI) reveal that this model [α-Hg(0)] reproduced the experimental spectrum well, with bond lengths within 0.01 Å of those reported for α-Hg(0).[38] The r-value, a measure of the goodness of the fit, was equal to 0.0270 (an r-value ≤ 0.05 typically indicates a good fit of a model to data[46]).

The FT-EXAFS spectra for all remaining samples exhibited peaks centered at ca. $R + \delta R$ = 2 Å, indicating the presence of

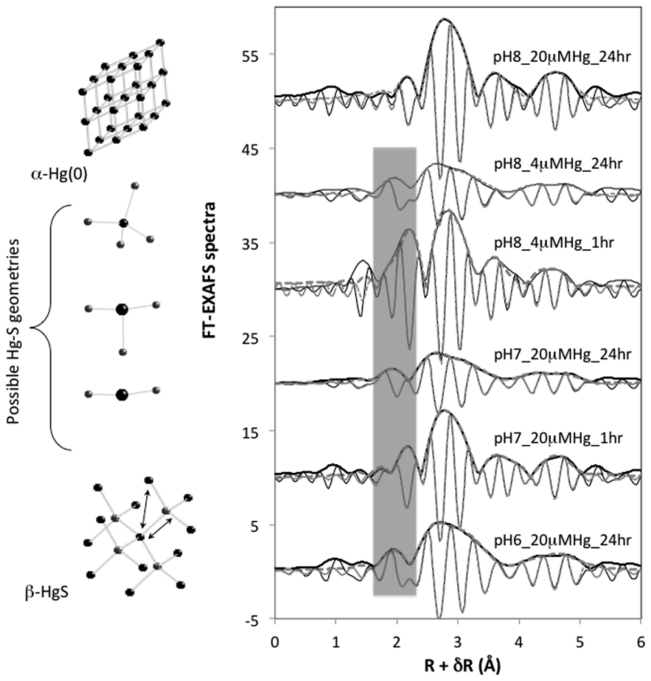

Figure 1. Magnitude (bold lines) and imaginary part (thin lines) of Fourier transforms of the EXAFS spectra (solid black lines) and fits to the data (dashed gray lines). The locations of the Hg(II)−S(-II) scattering paths are indicated by the gray box. Illustrations of α-Hg(0) and β-HgS are also provided; the black spheres depict Hg(II) and the gray spheres indicate S(-II). The arrows drawn on the β-HgS structure depict the Hg−S and Hg−S−Hg scattering paths used in modeling of the sample spectra. Also shown are illustrations of the Hg−S coordination geometries that are consistent with the bond distances obtained from fitting of the sample spectra.

anions neighboring the central Hg absorbing atom (Figure 1). Consequently, the EXAFS spectra could not be fitted satisfactorily with scattering paths from α-Hg(0) alone [r-values between 0.0937 and 0.1536 (data not shown)]. Only S and Hg backscatterers were expected to contribute to the sample EXAFS spectra, as there were no other elements in solution that could outcompete S(-II) for complexation with Hg(II). Furthermore, the location of the first peak in the FT-EXAFS spectra was consistent with bond lengths for Hg(II)−S(-II).[47] Thus, a model in which Hg(II) was coordinated to S(-II) was used in fitting the EXAFS spectra. The Debye−Waller factors for the Hg−Hg scattering paths and the S_0^2 value were constrained to equal those derived from fitting the spectrum of sample pH8_20μMHg_24h; this was necessary due to the large amount of overlap between all scattering paths in the FT-EXAFS spectra that otherwise led to large errors in the fitted parameters. The bond lengths (R, Å), coordination numbers (CN), and reference energies (E_0, eV) were not constrained. The Debye−Waller factors for the Hg-S scattering paths were unconstrained whenever possible; otherwise, they were set equal to the value obtained from fitting of the spectrum of sample pH7_20μMHg_1h (see the SI for further details of the fitting procedure).

The Hg(II)-S bond length varied widely among samples, from 2.30 ± 0.01 to 2.59 ± 0.01 Å (Table 1 and Figure 1), indicating that Hg(II) was coordinated to S(-II) in multiple geometries. Samples pH7_20μMHg_1h and pH6_20μMHg_24h exhibited coordination environments similar to that observed for β-HgS, in which sulfide ligands are coordinated to Hg at a distance of 2.53 Å.[36] Indeed, a Hg−Hg scattering path from β-HgS with an interatomic distance of 4.13 Å marginally improved the fit for sample pH7_20μMHg_24h when its CN was constrained, based on the geometry of the mineral, to equal three times the CN for the Hg−S scattering path. For sample pH8_4μMHg_24h, the Hg−S bond distance was slightly short (2.49 ± 0.03 Å) relative to β-HgS.

Sample pH7_20μMHg_24h exhibited a bond length (2.39 ± 0.02 Å) that was inconsistent with the structure of β-HgS, as did the sample pH8_4μMHg_1h, which was best fit with two Hg−S scattering paths: one at 2.30 ± 0.01 Å and one at 2.59 ± 0.01 Å. Trigonal Hg-thiol complexes with a T-shaped geometry have been reported previously[48] in which the "leg" of the T is much longer (e.g., by 0.4−0.5 Å) than the "arms" of the T. It is possible that the bonding environment in this sample (pH 8) is represented by a T-shaped complex; alternatively, it is possible that two distinct species existed corresponding to the two Hg−S distances.

Purgeable Hg Production. The concentrations of purgeable Hg evolved from samples containing FeS were significantly larger (p < 0.028 for all samples relative to the control using a two-tailed Student's t test) than those produced under control conditions (Figure 2). The fraction of Hg volatilized was <50% of the total Hg added to the initial FeS suspensions (20 μM), which is inconsistent with the results obtained using EXAFS spectroscopy (although it should be cautioned that EXAFS spectroscopy is not optimal for quantifying Hg(0); see SI). The discrepancy may arise if $Hg(0)_{(l)}$ forms (which is expected, since the solubility of $Hg(0)_{(l)}$ is 0.3 μM[49]), thus posing a kinetic limitation on the amount of Hg(0) removed from the suspensions, since $Hg(0)_{(l)}$ must dissolve to release $Hg(0)_{(g)}$. Previous studies have suggested that the formation of $Hg(0)_{(l)}$ by magnetite limited detection of $Hg(0)_{(g)}$ in the headspace of reactors.[43]

Although the concentration of purgeable Hg produced in samples buffered at pH 6 and 8 was monitored only under dark conditions, the concentration of purgeable Hg did not differ significantly (p = 0.60 using a two-tailed Student's t test) under illuminated versus dark conditions in samples buffered at pH 7 (Figure S5 of the SI) indicating that Hg(II) reduction occurred to a similar extent regardless of illumination. The amount of purgeable Hg produced in an unbuffered FeS suspension (pH = 6.0) was the same, within error, as the amount of purgeable Hg produced in the buffered FeS suspension (pH = 5.8) (Figure S6 of the SI). Thus, it may be concluded that purgeable Hg was generated from the reduction of Hg(II)−S(-II) by FeS under all experimental conditions we examined and its concentration was independent of whether light or organic buffering compounds were present.

■ DISCUSSION

Speciation of Hg(II) in Association with FeS. The dominant coordination environment inferred for Hg(II) in samples pH7_20μMHg_1h and pH6_20μMHg_24h was consistent with the bonding environment in β-HgS (indeed, it was possible to improve the EXAFS fit for sample pH7_20μMHg_1h by adding a Hg−Hg scattering path for β-HgS). Some fraction of Hg(II) may well have existed as β-HgS in all samples, since they were synthesized under conditions in which β-HgS is expected to be the most thermodynamically stable Hg(II)−S(-II) species. Studies by Skyllberg and Drott[24] and Jeong et al.[26] indicate that the primary interaction between

Table 1. Fitting Parameters for Samples Containing a Mixture of Hg(0) and Hg(II)[a]

sample	E_0 (eV)	scattering pair	R (Å)	CN	σ^2 (Å^2)	r-value
pH6_20μMHg_24h[b]	2.17 ± 1.73	Hg−S	2.51 ± 0.02	0.9 ± 0.1	0.0032	0.0046
		Hg−Hg1	2.99 ± 0.01	6.0 ± 0.4	0.0026	
		Hg−Hg2	3.45 ± 0.02	5.7 ± 0.9	0.0072	
		Hg−Hg3	4.55 ± 0.02	8.1 ± 1.8	0.0053	
		Hg−Hg4	4.89 ± 0.06	4.6 ± 3.5	0.0084	
pH7_20μMHg_24h[c]	1.38 ± 1.93	Hg−S	2.39 ± 0.02	1.2 ± 0.4	0.0093 ± 0.0033	0.0099
		Hg−Hg1	2.96 ± 0.01	3.4 ± 0.3	0.0025	
		Hg−Hg2	3.44 ± 0.02	4.4 ± 0.6	0.0070	
		Hg−Hg3	4.51 ± 0.02	5.1 ± 1.2	0.0053	
		Hg−Hg4	4.96 ± 0.05	4.4 ± 2.1	0.0084	
pH7_20μMHg_ h[d]	2.73 ± 1.39	Hg−S	2.51 ± 0.01	0.9 ± 0.3	0.0032 ± 0.0024	0.0086
		Hg−S−Hg	4.10 ± 0.03	2.6	0.0079 ± 0.0032	
		Hg−Hg1	2.98 ± 0.01	4.8 ± 0.2	0.0025	
		Hg−Hg2	3.46 ± 0.01	4.6 ± 0.7	0.0070	
		Hg−Hg3	4.56 ± 0.01	5.3 ± 1.4	0.0053	
		Hg−Hg4	4.90 ± 0.06	2.9 ± 2.9	0.0084	
pH8_4μMHg_24h[c]	3.60 ± 2.27	Hg−S	2.49 ± 0.03	1.8 ± 0.8	0.0118 ± 0.0051	0.0196
		Hg−Hg1	2.98 ± 0.02	3.8 ± 0.4	0.0025	
		Hg−Hg2	3.47 ± 0.03	3.9 ± 0.9	0.0070	
		Hg−Hg3	4.52 ± 0.03	6.0 ± 1.7	0.0053	
		Hg−Hg4	4.99 ± 0.07	3.8 ± 3.3	0.0084	
pH8_4μMHg_1h[b]	4.71 ± 1.57	Hg−S	2.30 ± 0.01	1.1 ± 0.2	0.0032	0.0199
		Hg−S	2.59 ± 0.01	1.6 ± 0.3	0.0032	
		Hg−Hg1	3.00 ± 0.01	5.5 ± 0.3	0.0025	
		Hg−Hg2	3.50 ± 0.01	5.3 ± 1.1	0.0070	

[a] S_0^2 = 0.80 for all samples. [b] k-Range = 3−10 Å^{-1}, R-range = 1.5−5.2. [c] k-Range = 3−10 Å^{-1}, R-range = 1−5.2 Å. [d] k-Range = 3−12 Å^{-1}, R-range = 1−5 Å.

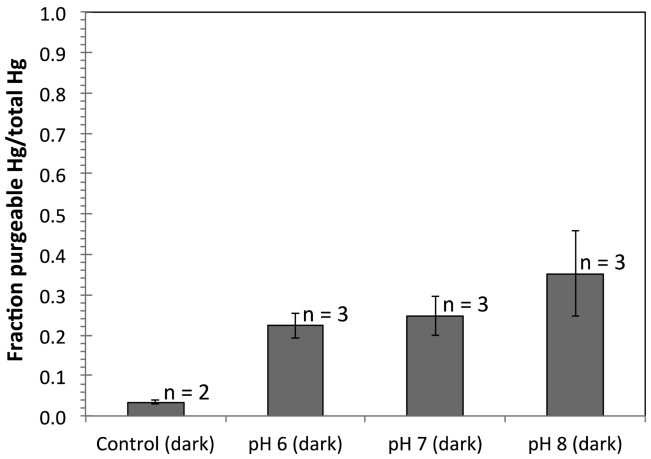

Figure 2. Purgeable Hg production in control solutions (left most column) and FeS suspensions (columns 2−4). The number of replicate samples (n) is provided in the plot. The error bars denote one standard deviation based on the average of the n replicates. The control contained 10 mM HEPES buffer and 20 μM Hg(II); "pH 6 (dark)" contained 10 mM MES buffer, 1 g/L FeS and 20 μM Hg; "pH 7 (dark)" contained 10 mM HEPES buffer, 1 g/L FeS and 20 μM Hg; "pH8 (dark)" contained 10 mM Tris buffer, 1 g/L FeS and 20 μM Hg. All samples and controls were equilibrated for 24 h.

FeS and Hg(II) is the dissolution of FeS in favor of the more stable β-HgS, a scenario similar to that described by Hyland et al.[50] for the reaction between PbS (galena) and soluble Hg(II).

However, the Hg−S bond lengths obtained from fitting of the spectra of samples pH7_20μMHg_24h (2.39 Å), pH8_4μMHg_24h (2.49 Å), and pH8_4μMHg_1h (2.30 and 2.59 Å) were not consistent with the formation of β-HgS. We interpret this inconsistency to mean that a mixture of Hg−S species forms with bond distances averaging to yield the fitted values, which is possible if the Hg(II)-S bond lengths are the same within the resolution (ΔR) of the FT-EXAFS spectra (ΔR = 0.17 or 0.22 Å for k-range = 3−10 Å^{-1} or k-range = 3−12 Å^{-1}, respectively[46]). The Debye−Waller factors of samples with bond distances intermediate between 2.30 and 2.51 Å were large [0.0093 Å^2 (pH7_20μMHg_24h) and 0.0118 Å^2 (pH8_4μMHg_24h) compared to 0.0035 Å^2 (sample pH7_20μMHg_1h)]. Such large Debye−Waller factors are consistent with a mixture of bonding environments. Support for our interpretation also comes from principal component analysis (PCA), which showed that only three components were required to reproduce the sample spectra (Figures S10−S12 of the SI); whereas five components would have been required if the samples contained three different species in addition to α-Hg(0) and β-HgS. Lastly, the fact that the fitted average bond distances did not vary with the experimental parameters examined (pH, initial Hg(II) concentration, reaction time) is also consistent with mixtures of similar species occurring under all experimental conditions, rather than a single species being favored under any one experimental condition.

Unlike Skyllberg and Drott,[24] who found that all Hg(II) formed β-HgS when reacted with FeS, Jeong et al.[25] and Wolfenden et al.[23] also observed that their EXAFS spectra reflected coordination environments that were not consistent with β-HgS. Jeong et al.[25] postulated that a fraction of the Hg(II) formed a complex with the FeS surface and fit their EXAFS spectra with a shell of Cl atoms at 2.48−2.50 Å (note that EXAFS spectroscopy cannot be used to distinguish between Cl and S atoms). Inclusion of a second species in

their model was supported by improved agreement between the experimental and fitted spectra and by identification (via high-angle annular dark field-scanning transmission electron microscopy) of a diffuse layer of Hg associated with FeS particles in addition to localized "hot spots" of Hg attributed to β-HgS nanoparticles.[25] Wolfenden et al.[23] fit their EXAFS spectra with a Hg(II)-S scattering path at 2.38 Å. This bond length is consistent with the presence of α-HgS, however there was no higher-order structure in the FT-EXAFS spectra attributable to scattering from α-HgS. Furthermore, β-HgS is expected to precipitate from solutions of Hg(II) and S(-II) at room temperature.[51] The Hg(II)-S bond lengths identified in our study span the range observed in these three studies (with the exception of pH8_4μMHg_1h), and the Hg:FeS molar ratios ($4 \times 10^{-4} - 2 \times 10^{-3}$) we investigated were intermediate between those investigated by Wolfenden et al.[23] (2×10^{-4}), Skyllberg and Drott[24] (1×10^{-3} to 2×10^{-3}), and Jeong et al.[25] (4×10^{-2} to 9×10^{-2}).

It is pertinent to note the similarity between the Hg(II)−S bond lengths obtained in our study and those obtained for Hg(II) reacted with organic matter or organic matter and S(-II). Slowey[52] suggested that nanoparticulate β-HgS, which formed when S(-II) was added to Hg-reacted dissolved organic matter, exhibited shortened bond distances (2.38−2.48 Å) as a result of a large number of undersaturated Hg(II) atoms at the surface of very small particles and from lattice strain induced by interactions with organic moieties at the surface of the HgS particles.[53] Similarly, Nagy et al.[54] suggested that Hg(II) formed Hg_xS_3 clusters when Hg(II) was reacted with soil organic matter, characterized by two Hg(II)−S bond lengths of 2.34−2.35 Å, one Hg(II)−S bond length of 2.54−2.57 Å, and x Hg−Hg bond lengths at 4.12−4.14 Å (note the similarity, in particular, between these fitted bond lengths and those obtained for the sample pH8_4μMHg_1h).

It may be that the variability in Hg(II)−S(-II) bond lengths obtained for our samples arose from heterogeneous precipitation of β-HgS, or, similarly, formation of tetrahedral Hg(II)−S(-II) clusters associated with the surface of FeS. Association with the FeS surface could induce distortions in the Hg(II)−S(-II) coordination environment[53] such that the average Hg(II)−S(-II) distance is not always characteristic of Hg−S tetrahedra. It is not possible to identify unambiguously the bonding environments of the Hg(II)−S(-II) species; however, it is possible to say that many of the fitted bond lengths were inconsistent with homogeneous precipitation of β-HgS, which suggests that Hg(II) was associated with the FeS surface in some way.

Reduction of Hg(II)−S(-II) by FeS. Previous researchers who have investigated the reactions between Hg(II) and FeS (with Hg:FeS < 1) have been unable to detect Hg(0) using molecular-scale techniques. This may have occurred because the detection of Hg(0) is sensitive to the preparation and preservation of samples for spectroscopic analysis. For instance, Jew et al.[44] observed that Hg(0) was detectable in their sample spectra collected at 77 K, even though it went undetected when spectra of the same samples were collected at room temperature. Furthermore, Jew et al.[44] found it necessary to cool their α-Hg(0) reference slowly, because rapid quenching resulted in a glass that exhibited reduced EXAFS oscillations relative to crystalline α-Hg(0). Skyllberg and Drott[24] and Jeong et al.[25] dried their filtered Hg-reacted FeS suspensions in a glovebox, from which any Hg(0) that was formed could have escaped. Jeong et al.,[25] recognizing this problem, also performed XANES spectroscopy on wet, Hg-reacted FeS samples and were still unable to detect Hg(0). However, their XANES spectra were collected at room temperature[25] at which Hg(0) is highly volatile relative to its volatility at both 77 and 10 K.[55] We were able to detect Hg(0) consistently using EXAFS spectroscopy only if samples were frozen at −15 °C; spectra from wet samples preserved at temperatures of approximately 20 °C (and measured at 77 K) did not always exhibit scattering from Hg(0) that was above the detection limit of EXAFS spectroscopy (Figure S13 of the SI), possibly due to evolution of $Hg(0)_{(g)}$ or formation of Hg(0) glass upon cooling. Finally, Hg(0) was not produced in our experiments by beam damage. Although sample preservation and the temperature of EXAFS spectra collection impact detection of Hg(0), differences in the chemistry of the suspensions employed by different researchers also may enhance or diminish Hg(0) formation.

Mercury(II) can be reduced abiotically, in particular, by mixed Fe(II)−Fe(III) mineral phases and organic matter.[41,56,57] However, in many studies, Hg existed in solution as either a hydroxy- or chloro-complex, which are weak compared to the S(-II) complexes of Hg (e.g., Skyllberg[14]). Indeed, Mishra et al.[58] observed that Hg(II) reduction by both magnetite and green rust was severely diminished in the presence of the sulfhydryl groups associated with bacterial biomass. Furthermore, researchers have demonstrated that Hg(0) can be oxidized when it binds to thiol groups in organic matter,[59,60] bacterial cells,[11,61] or cell exudates.[61] Similarly, oxidation of Hg(0) due to S(-II) complexation has also been observed after reaction with PbS.[62] Thus, it appears that non-S(-II) complexes of Hg(II) may be available for reduction, whereas strong Hg(II)−S(-II) complexes are not, and instead actually favor the oxidation of Hg(0) in the absence of a powerful reductant. In contrast, Hg(II)−S(-II) complexes dominate Hg speciation in both the solid and aqueous phases in FeS suspensions, yet the EXAFS spectrum is dominated by scattering from α-Hg(0) after only 1 h of reaction. A fraction of the Hg(II) added to the suspension remained divalent under most of the experimental conditions examined. It is likely that these species were kinetically recalcitrant, but thermodynamically unstable relative to Hg(0). Our identification of non-β-HgS coordination environments is consistent with the formation of metastable Hg(II) species.

Thus, we propose that reduction of Hg(II)−S(-II) by FeS is thermodynamically favorable in natural sediments. Thermodynamic modeling of Hg speciation under our experimental conditions (assuming β-HgS precipitates) predicts that Hg(II) will be converted to Hg(0) between pe = −2 and pe = −3.5 (Table S6 and Figure S14). One of the difficulties facing a thermodynamic description of the oxidation of FeS in our system is the absence of formation of crystalline end-products for which equilibrium information is available,[30] which limits our ability to calculate accurate reduction potentials for FeS/Fe(III) or FeS/oxidized S couples and, consequently, to develop pe−pH diagrams for FeS in our system.

Kirsch et al.[16] circumvented this difficulty through careful measurement of the electron activity in their FeS suspensions, which also spanned that over which we expect Hg(II) to be reduced. The authors[16] observed that reduction of Pu(V) occurred in FeS suspensions initially buffered at pe between −5.2 and −5.7 (pe was measured in the mineral suspension and in the supernatant solution above the pelleted mineral, respectively). Over the course of the reaction, Pu(IV) and

Pu(III) formed and pe increased to between −4.9 and −2.1 (measured in the mineral suspension and in the supernatant solution, respectively).

There is no consensus in the literature regarding which redox-active element, S(-II) (e.g.,[15,63]) or Fe(II) (e.g.,[16,64,65]), is oxidized when metals or metalloids are reduced. Furthermore, FeS is much more soluble than Fe(II) oxides or mixed Fe(II)−Fe(III) oxides,[29] so aqueous Fe(II) and S(-II) could potentially transfer electrons as well. Indeed, Hyun et al.[15] suggested that S(-II) in equilibrium with FeS was responsible for reduction of U(VI). However, oxidized Fe and S species are almost always detected in FeS suspensions together[64,66−68] and, to our knowledge, no analysis of the kinetics of reduction of contaminants by FeS has been performed that would allow a mechanism of electron transfer to be suggested.

Mackinawite's capacity to act as a powerful reductant can be rationalized by the presence of short Fe−Fe bonds that are postulated to be metallic.[69] Kwon and colleagues[70] used density functional theory to derive the density of states for FeS and found that the Fermi level was populated by Fe 3d electrons. In support of their interpretation that Fe 3d electrons were highly delocalized, the authors[70] presented an Fe $L_{2,3}$-edge X-ray absorption spectrum for FeS which was more like the spectrum of metallic Fe (α-Fe) than the isostructural Fe mineral ($SmO_{0.85}FeAs$). This predicted metallic character of the Fe−Fe bonds[69,70] in FeS suggests that the electrons for reduction originate from Fe(II).

Additionally, aqueous Fe(II) in equilibrium with FeS may act as an electron donor. For instance, hydroxylated Fe(II) species have been implicated in Hg(II) reduction (although not in sulfidic suspensions[71]). Due to the large concentrations of aqueous Fe(II) in our suspensions (ca. 400−1000 μM), it is possible that aqueous Fe(II) complexes participated in the reduction of Hg(II), although our methodology did not allow us to determine whether there was a relationship between the concentration of Fe(II) in solution and the amount of Hg(0) produced.

There are few studies of Hg(0) concentrations in anoxic sediments,[13] but the results of our work suggest that Hg(0) may account for a significant fraction of the total Hg in wetland, estuarine, lake, or aquifer sediments, in agreement with the finding of Bouffard and Amyot[13] that up to 28% of the total Hg in anoxic lake sediments is Hg(0). The production of Hg(0) by FeS in anoxic sediments should significantly impact the biogeochemical cycling of Hg in these environments. Reduction of Hg(II)−S(-II) by FeS could compete with the oxidation of Hg(0) by organic matter[59,60,72] (and thiol groups on bacterial cells[11,61]) and of course with the methylation of Hg(II), thereby limiting subsequent toxicity.

■ ASSOCIATED CONTENT

Supporting Information

Thermodynamic calculations of Hg(II) speciation and Hg(0) production as measured by CVAFS under control conditions. Wet-chemical, X-ray scattering, and spectroscopic characterization of the FeS substrate. Details of the EXAFS fitting process. Comparison of FT-EXAFS spectra obtained for the same sample conditions when the sample was preserved at different temperatures. Lastly, thermodynamic simulations of the fraction of Hg(0) generated as a function of pe. This material is available free of charge via the Internet at http://pubs.acs.org.

■ AUTHOR INFORMATION

Corresponding Author

*E-mail: shbone@slac.stanford.edu. Tel.: (650) 926-2990. Current mailing address: Stanford Synchrotron Radiation Lightsource, SLAC, 2575 Sand Hill Road, Menlo Park, California 94025, United States.

Notes

The authors declare no competing financial interest.

■ ACKNOWLEDGMENTS

Portions of this research were carried out at the Stanford Synchrotron Radiation Lightsource, a Directorate of SLAC National Accelerator Laboratory and an Office of Science User Facility operated for the U.S. Department of Energy of Science by Stanford University. The SSRL Structural Molecular Biology Program is supported by the DOE Office of Biological and Environmental Research, and by the National Institutes of Health, National Institute of General Medical Sciences (including P41GM103393). The contents of this publication are solely the responsibility of the authors and do not necessarily represent the official views of NIGMS or NIH. This research was supported by the Director, Office of Energy Research, Office of Basic Energy Sciences, of the U.S. Department of Energy under Contract No. DE-AC02-05CH11231 at Lawrence Berkeley National Laboratory. This research was funded in part by the Esper Larsen Jr. Fund (Department of Earth & Planetary Science, UC Berkeley) through the project, "Preventing Mercury Methylation in Estuarine Porewaters: Role of the Iron Sulfide Mineral Mackinawite." S.B. was also supported during the completion of this research by a Ludo Frevel Crystallography Fellowship from the International Centre for Diffraction Data and by the University of California through a Toxic Substances Teaching and Research Program Student Fellowship, a Jane Lewis Fellowship, and a James Bennett Agricultural Fellowship. S.B. was also supported during the completion of this manuscript by the SLAC SFA program (project number 10094).

■ REFERENCES

(1) Fitzgerald, W. F.; Engstrom, D. R.; Mason, R. P.; Nater, E. A. The case for atmospheric mercury contamination in remote areas. *Environ. Sci. Technol.* **1998**, *32* (1), 1−7, DOI: 10.1021/es970284w.

(2) Parks, J. M.; Johs, A.; Podar, M.; Bridou, R.; Hurt, R. A.; Smith, S. D.; Tomanicek, S. J.; Qian, Y.; Brown, S. D.; Brandt, C. C.; Palumbo, A. V.; Smith, J. C.; Wall, J. D.; Elias, D. A.; Liang, L. The Genetic Basis for Bacterial Mercury Methylation. *Science* **2013**, DOI: 10.1126/science.1230667.

(3) Hsu-Kim, H.; Kucharzyk, K. H.; Zhang, T.; Deshusses, M. A. Mechanisms Regulating Mercury Bioavailability for Methylating Microorganisms in the Aquatic Environment: A Critical Review. *Environ. Sci. Technol.* **2013**, DOI: 10.1021/es304370g.

(4) Lin, C.; Yee, N.; Barkay, T. Microbial transformations in the mercury cycle. In *Environmental Chemistry and Toxicology of Mercury*; Liu, G.; Cai, Y.; O'Driscoll, N. J., Eds; John Wiley & Sons: Hoboken, NJ, 2012; pp 155−192.

(5) Barkay, T.; Gillman, M.; Turner, R. R. Effects of dissolved organic carbon and salinity on bioavailability of mercury. *Appl. Environ. Microbiol.* **1997**, *63* (11), 4267−4271, DOI: 10.1016/j.envpol.2007.12.004.

(6) Benoit, J. M.; Gilmour, C. C.; Mason, R. P.; Heyes, A. Sulfide controls on mercury speciation and bioavailability to methylating bacteria in sediment pore waters. *Environ. Sci. Technol.* **1999**, *33* (6), 951−957, DOI: 10.1021/es9808200.

(7) Benoit, J. M.; Mason, R. P.; Gilmour, C. C. Estimation of mercury-sulfide speciation in sediment pore waters using octanol-water partitioning and implications for availability to methylating bacteria. *Environ. Toxicol. Chem.* **1999**, *18* (10), 2138−2141, DOI: 10.1002/etc.5620181004.
(8) Schaefer, J. K.; Morel, F. M. M. High methylation rates of mercury bound to cysteine by Geobacter sulfurreducens. *Nat. Geosci.* **2009**, *2* (2), 123−126, DOI: 10.1038/ngeo412.
(9) Schaefer, J. K.; Rocks, S. S.; Zheng, W.; Liang, L. Y.; Gu, B. H.; Morel, F. M. M. Active transport, substrate specificity, and methylation of Hg(II) in anaerobic bacteria. *Proc. Natl. Acad. Sci. U. S. A.* **2011**, *108* (21), 8714−8719, DOI: 10.1073/pnas.1105781108.
(10) Zhang, T.; Kim, B.; Leyard, C.; Reinsch, B. C.; Lowry, G. V.; Deshusses, M. A.; Hsu-Kim, H. Methylation of mercury by bacteria exposed to dissolved, nanoparticulate, and microparticulate mercuric sulfides. *Environ. Sci. Technol.* **2012**, *46* (13), 6950−6958, DOI: 10.1021/es203181m.
(11) Colombo, M. J.; Ha, J.; Reinfelder, J. R.; Barkay, T.; Yee, N. Anaerobic oxidation of Hg(0) and methylmercury formation by *Desulfovibrio desulfuricans* ND132. *Geochim. Cosmochim. Acta* **2013**, *112*, 166−177, DOI: 10.1016/j.gca.2013.03.001.
(12) Morel, M. M.; Hering, J. G. *Principles and applications of aquatic chemistry*. Wiley: New York, 1993.
(13) Bouffard, A.; Amyot, M. Importance of elemental mercury in lake sediments. *Chemosphere* **2009**, *74*, 1098−1103, DOI: 10.1016/j.chemosphere.2008.10.045.
(14) Skyllberg, U. Competition among thiols and inorganic sulfides and polysulfides for Hg and MeHg in wetland soils and sediments under suboxic conditions: Illumination of controversies and implications for MeHg net production. *J. Geophys. Res.: Biogeosci.* **2008**, DOI: G00c03 10.1029/2008jg000745.
(15) Hyun, S. P.; Davis, J. A.; Sun, K.; Hayes, K. F. Uranium(VI) Reduction by Iron(II) Monosulfide Mackinawite. *Environ. Sci. Technol.* **2012**, *46* (6), 3369−3376, DOI: 10.1021/es203786p.
(16) Kirsch, R.; Fellhauer, D.; Altmaier, M.; Neck, V.; Rossberg, A.; Fanghanel, T.; Charlet, L.; Scheinost, A. C. Oxidation State and Local Structure of Plutonium Reacted with Magnetite, Mackinawite, and Chukanovite. *Environ. Sci. Technol.* **2011**, *45* (17), 7267−7274, DOI: 10.1021/es200645a.
(17) Hammerschmidt, C. R.; Fitzgerald, W. F.; Balcom, P. H.; Visscher, P. T. Organic matter and sulfide inhibit methylmercury production in sediments of New York/New Jersey Harbor. *Mar. Chem.* **2008**, *109* (1−2), 165−182, DOI: 10.1016/j.marchem.2008.01.007.
(18) Han, S.; Obraztsova, A.; Pretto, P.; Choe, K. Y.; Gieskes, J.; Deheyn, D. D.; Tebo, B. M. Biogeochemical factors affecting mercury methylation in sediments of the Venice Lagoon, Italy. *Environ. Toxicol. Chem.* **2007**, *26* (4), 655−663, DOI: 10.1897/06-392r.1.
(19) Mason, R. P.; Reinfelder, J. R.; Morel, F. M. M. Uptake, toxicity, and trophic transfer of mercury in a coastal diatom. *Environ. Sci. Technol.* **1996**, *30* (6), 1835−1845, DOI: 10.1021/es950373d.
(20) Mehrotra, A. S.; Horne, A. J.; Sedlak, D. L. Reduction of net mercury methylation by iron in Desulfobulbus propionicus (1pr3) cultures: Implications for engineered wetlands. *Environ. Sci. Technol.* **2003**, *37* (13), 3018−3023, DOI: 10.1021/es0262838.
(21) Mehrotra, A. S.; Sedlak, D. L. Decrease in net mercury methylation rates following iron amendment to anoxic wetland sediment slurries. *Environ. Sci. Technol.* **2005**, *39* (8), 2564−2570, DOI: 10.1021/es049096d.
(22) Han, S.; Obraztsova, A.; Pretto, P.; Deheyn, D. D.; Gieskes, J.; Tebo, B. M. Sulfide and iron control on mercury speciation in anoxic estuarine sediment slurries. *Mar. Chem.* **2008**, *111*, 214−220, DOI: 10.1016/j.marchem.2008.05.002.
(23) Wolfenden, S.; Charnock, J. M.; Hilton, J.; Livens, F. R.; Vaughan, D. J. Sulfide species as a sink for mercury in lake sediments. *Environ. Sci. Technol.* **2005**, *39* (17), 6644−6648, DOI: 10.1021/es048874z.
(24) Skyllberg, U.; Drott, A. Competition between disordered iron sulfide and natural organic matter associated thiols for mercury(II)-An EXAFS study. *Environ. Sci. Technol.* **2010**, *44*, 1254−1259, DOI: 10.1021/es902091w.
(25) Jeong, H. Y. S. K.; Hayes, K. F. Microscopic and spectroscopic characterization of Hg(II) immobilization by mackinawite. *Environ. Sci. Technol.* **2010**, *44* (19), 7476−7483, DOI: 10.1021/es100808y.
(26) Jeong, H. Y.; Klaue, B.; Blum, J. D.; Hayes, K. F. Sorption of mercuric ion by synthetic nanocrystalline mackinawite (FeS). *Environ. Sci. Technol.* **2007**, *41* (22), 7699−7705, DOI: 10.1021/es070289l.
(27) EPA Method 376.1: *Sulfide by Titrimetry*; U.S. Environmental Protection Agency; Washington, DC; http://www.epa.gov/fem/methcollectns.htm.
(28) Viollier, E.; Inglett, P. W.; Hunter, K.; Roychoudhury, A. N.; Van Cappellen, P. The ferrozine method revisited: Fe(II)/Fe(III) determination in natural waters. *Appl. Geochem.* **2000**, *15* (6), 785−790, DOI: 10.1016/s0883-2927(99)00097-9.
(29) Rickard, D.; Luther, G. W. Chemistry of iron sulfides. *Chem. Rev.* **2007**, *107* (2), 514−562, DOI: 10.1021/cr0503658.
(30) Bone, S. E. Mechanisms of Mercury Sequestration by Mackinawite (Tetragonal FeS). Ph.D. Dissertation, University of California, Berkeley, CA, 2013.
(31) Fitzgerald, W. F. L.; Hammerschmidt, C. H.; Marine, C. M. Biogeochemistry of Mercury. *Chem. Rev.* **2007**, *107* (2), 641−662, DOI: 10.1021/cr050353m.
(32) Schecher, W. M. D. *MINEQL+: A Chemical Equilibrium Modeling System*, 4.5; Environmental Research Software: Hallowell, ME, 1998.
(33) Webb, S. M. SIXPack: a graphical user interface for XAS analysis using IFEFFIT. *Phys. Scr.* **2004**, *T115*, 1011−1014, DOI: 10.1238/Physica.Topical.115a01011.
(34) Newville, M.; Livins, P.; Yacoby, Y.; Rehr, J. J.; Stern, E. A. Near edeg X-ray absorption fine structure of Pb- a comparison of theory and experiment. *Phys. Rev. B* **1993**, *47* (21), 14126−14131, DOI: 10.1103/PhysRevB.47.14126.
(35) Newville, M. EXAFS analysis using FEFF and FEFFIT. *J. Synchrotron Radiat.* **2001**, *8*, 96−100, DOI: 10.1107/S0909049500016290.
(36) Wycoff, R. W. G. *Crystal Structures 1*, 2nd ed.; Interscience Publishers: New York, NY, 1963.
(37) Auvrey, P.; Genet, F. Affinement de la structure cristalline du cinabre a-HgS. *Bull. Soc. Fr. Mineral. Cristallogr.* **1973**, *96*, 218−219.
(38) Barrett, C. S. The structure of mercury at low temperatures. *Acta Crystallogr.* **1957**, *10*, 58−60, DOI: 10.1107/S0365110X57000134.
(39) Amyot, M.; Mierle, G.; Lean, D. R. S.; McQeen, D. Sunlight-induced formation of dissolved gaseous mercury in lake waters. *Environ. Sci. Technol.* **1994**, *28*, 2366−2371, DOI: 10.1021/es00062a022.
(40) Buchholz, A.; Laskov, C.; Haderlein, S. B. Effects of Zwitterionic Buffers on Sorption of Ferrous Iron at Goethite and Its Oxidation by CCl4. *Environ. Sci. Technol.* **2011**, *45* (8), 3355−3360, DOI: 10.1021/es103172c.
(41) Wiatrowski, H. A.; Das, S.; Kukkadapu, R.; Ilton, E. S.; Barkay, T.; Yee, N. Reduction of Hg(II) to Hg(0) by Magnetite. *Environ. Sci. Technol.* **2009**, *43* (14), 5307−5313, DOI: 10.1021/es9003608.
(42) EPA Method 1631, Revision E. *Mercury in water by oxidation, purge and trap, and cold vapor atomis flourescence spectrometry*; U.S. Environmental Protection Agency: Washington, DC, 2002; http://water.epa.gov/scitech/methods/cwa/metals/mercury/index.cfm.
(43) Pasakarnis, T. S.; Boyanov, M. I.; Kemner, K. M.; Mishra, B.; O'Loughlin, E. J.; Parkin, G.; Scherer, M. M. Influence of Chloride and Fe(II) Content on the Reduction of Hg(II) by Magnetite. *Environ. Sci. Technol.* **2013**, *47* (13), 6987−6994, DOI: 10.1021/es304761u.
(44) Jew, A. D.; Kim, C. S.; Rytuba, J. J.; Gustin, M. S.; Brown, G. E. New technique for quantification of elemental Hg in mine wasted and its implications for mercury evasion into the atmosphere. *Environ. Sci. Technol.* **2011**, *45*, 412−417, DOI: 10.1021/es1023527.
(45) Calvin, S. Relationship between electron delocalization and asymmetry of the pair distribution function as determined by X-ray

absorption spectroscopy. Ph.D. Dissertation. The City University of New York, New York, 2001.
(46) Kelly, S. D.; Hesterberg, D.; Ravel, B. Analysis of soild and minerals using X-ray absorption spectroscopy. In *Methods of Soil Analysis, Part 5: Mineralogical Methods*; Ulrey, A. L., Drees, R. L., Eds; Soil Science Society of America: Madison, WI, 2008; pp 387−464.
(47) Grdenic, D. Structural Chemistry of Mercury. *Q. Rev., Chem. Soc.* **1965**, *19* (3), 303−328, DOI: 10.1039/qr9651900303.
(48) Manceau, A.; Nagy, K. L. Relationships between Hg(II)-S bond distance and Hg(II) coordination in thiolates. *Dalton Trans.* **2008**, *11*, 1421−1425, DOI: 10.1039/b718372k.
(49) Morel, F. M. M.; Hering, J. G. *Principles and Applications of Aquatic Chemistry*; Wiley-Interscience, 1993.
(50) Hyland, M. M.; Jean, G. E.; Bancroft, G. M. XPS and AES studies of Hg(II) sorption and desorption reactions on sulphide minerals. *Geochim. Cosmochim. Acta* **1990**, *54*, 1957−1967, DOI: 10.1016/0016-7037(90)90264-L.
(51) Charnock, J. M.; Moyes, L. N.; Pattrick, R. A. D.; Mosselmans, J. F. W.; Vaughan, D. J.; Livens, F. R. The structural evolution of mercury sulfide precipitate: an XAS and XRD study. *Am. Mineral.* **2003**, *88* (8−9), 1197−1203, DOI: 10.1180/minmag.2010.074.1.85.
(52) Slowey, A. J. Rate of formation and dissolution of mercury sulfide nanoparticles: the dual role of natural organic matter. *Geochim. Cosmochim. Acta* **2010**, *74*, 4693−4708, DOI: 10.1016/j.gca.2010.05.012.
(53) Gilbert, B.; Huang, F.; Lin, Z.; Goodell, C.; Zhang, H. Z.; Banfield, J. F. Surface chemistry controls crystallinity of ZnS nanoparticles. *Nano Lett.* **2006**, *6* (4), 605−610, DOI: 10.1021/nl052201c.
(54) Nagy, K. L.; Manceau, A.; Gasper, J. D.; Ryan, J. N.; Aiken, G. R. Metallothionein-like multinuclear clusters of mercury(II) and sulfur in peat. *Environ. Sci. Technol.* **2011**, *45*, 7298−7306, DOI: 10.1021/es201025v.
(55) *The vapor pressure of mercury*; National Institute of Standards and Technology: Boulder, Co, 2006; www.physics.rutgers.edu/~eandrei/389/NISTIR.6643.pdf.
(56) Charlet, L.; Bosbach, D.; Peretyashko, T. Natural attenuation of TCE, As, Hg linked to the heterogeneous oxidation of Fe(II): an AFM study. *Chem. Geol.* **2002**, *190* (1−4), 303−319, DOI: 10.1016/S0009-2541(02)00122-5.
(57) O'Loughlin, E. J.; Kelly, S. D.; Kemner, K. M.; Csencsits, R.; Cook, R. E. Reduction of Ag(I), Au(II), Cu(II), and Hg(II) by Fe(II)/Fe(III) hydroxysulfate green rust. *Chemosphere* **2003**, *53*, 437−446, DOI: 10.1016/S0045-6535(03)00545-9.
(58) Mishra, B.; O'Loughlin, E. J.; Boyanov, M. I.; Kemner, K. M. Binding of Hg-II to High-Affinity Sites on Bacteria Inhibits Reduction to Hg-0 by Mixed Fe-II/III Phases. *Environ. Sci. Technol.* **2011**, *45* (22), 9597−9603, DOI: 10.1021/es201820c.
(59) Zheng, W.; Liang, L.; Gu, B. Mercury reduction and oxidation by reduced natural organic matter in anoxic environments. *Environ. Sci. Technol.* **2012**, *46*, 292−299, DOI: 10.1021/es203402p.
(60) Zheng, W.; Lin, H.; Mann, B. F.; Liang, L.; Gu, B. Oxidation of dissolved elemental mercury by thiol compounds under anoxic conditions. *Environ. Sci. Technol.* **2013**, *47* (22), 12827−12834, DOI: 10.1021/es402697u.
(61) Hu, H. Y.; Lin, H.; Zheng, W.; Tomanicek, S. J.; Johs, A.; Feng, X. B.; Elias, D. A.; Liang, L. Y.; Gu, B. H. Oxidation and methylation of dissolved elemental mercury by anaerobic bacteria. *Nat. Geosci.* **2013**, *6* (9), 751−754, DOI: 10.1038/ngeo1894.
(62) Genin, F.; Alnot, M.; Ehrhardt, J. Interaction of vapours of mercury with PbS(001): a study by X-ray photoelectron spectroscopy, RHEED and X-ray absorption spectroscopy. *Appl. Surf. Sci.* **2001**, *173*, 44−53, DOI: 10.1016/S0169-4332(00)00874-6.
(63) Widler, A. M.; Seward, T. M. The adsorption of gold(I) hydrosulfide complexes by iron sulfide surfaces. *Geochim. Cosmochim. Acta* **2002**, *66* (3), 383−402.
(64) Kirsch, R. S.; Rossberg, A.; Banerjee, D.; Charlet, L. Reduction of antimony by nano-particulate magnetite and mackinawite. *Mineral. Mag.* **2008**, *72* (1), 27−31, DOI: 10.1180/minmag.2008.072.1.185.
(65) Patterson, R. R.; Fendorf, S.; Fendorf, M. Reduction of hexavalent chromium by amorphous iron sulfide. *Environ. Sci. Technol.* **1997**, *31* (7), 2039−2044, DOI: 10.1021/es960836v.
(66) Mullet, M.; Boursiquot, S.; Abdelmoula, M.; Genin, J.; Ehrhardt, J. Surface chemistry and structural properties of mackinawite prepared by reaction of sulfide ions with metallic iron. *Geochim. Cosmochim. Acta* **2002**, *66* (5), 829−836, DOI: 10.1016/S0016-7037(01)00805-5.
(67) Li, Y.; van Santen, R. A.; Weber, T. High-tempurature FeS-FeS2 solid-state transitions: Reactions of solid mackinawite with gaseous H2S. *J. Solid State Chem.* **2008**, *181*, 3151−3162, DOI: 10.1016/j.jssc.2008.08.024.
(68) Herbert, R. B.; Benner, S. G.; Pratt, A. R.; Blowes, D. W. Surface chemistry and morphology of poorly crystalline iron sulfides precipitated in media containing sulfate-reducing bacteria. *Chem. Geol.* **1998**, *144* (1−2), 87−97, DOI: 10.1016/S0009-2541(97)00122-8.
(69) Vaughan, D.; Ridout, M. S. Mossbauer studies of some sulphide minerals. *J. Inorg. Nucl. Chem.* **1971**, *33* (3), 741−746, DOI: 10.1016/0022-1902(71)80472-4.
(70) Kwon, K. D.; Refson, K.; Bone, S. E.; Qiao, R.; Yang, W.; Liu, Z.; Sposito, G. Magnetic ordering in mackinawite (tetragonal FeS): Evidence for strong itinerant spin fluctuations. *Phys. Rev. B* **2011**, *83* (064402), 1−7, DOI: 10.1103/PhysRevB.83.064402.
(71) Amirbahman, A.; Kent, D. B.; Curtis, G. P.; Marvin-DiPasquale, M. C. Kinetics of Homogeneous and Surface-Catalyzed Mercury(II) Reduction by Iron(II). *Environ. Sci. Technol.* **2013**, *47* (13), 7204−7213, DOI: 10.1021/es401459p.
(72) Gu, B.; Bian, Y.; Miller, C. L.; DOng, W.; Jiang, X.; Liang, L. Mercury reduction and complexation by natural organic matter in anoxic environments. *Proc. Natl. Acad. Sci. U.S.A.* **2011**, *108* (4), 1479−1483, DOI: 10.1073/pnas.1008747108.